Manuscript refereed by Dr Bjoern Hoschke (Kennametal Shared Services GmbH, Germany)

Micromechanics of Ti(C,N)-Feni Composites: Statistical Analysis and Flow Stress Determination for the Feni Binder

H. Besharatloo [1,2,*], J.J. Roa [1,2], M. Dios[3], A. Mateo [1,2], B. Ferrari[4], E. Gordo[3] and L. Llanes [1,3]

[1] CIEFMA-Departament de Ciència dels Materials i Enginyeria Metal·lúrgica, EEBE, Universitat Politècnica de Catalunya, 08019 Barcelona, Spain
[2] Universitat Politècnica de Catalunya, Research Center in Multiscale Science and Engineering, Campus Diagonal Besòs - Edif. DBC, Av. d'Eduard Maristany, 10-14, 08019 Barcelona, Spain
[3] GTP – Universidad Carlos III Madrid, Leganés 28911, Spain
[4] ICV-CSIC, Madrid 28049, Spain
*Corresponding author e-mail address: hossein.besharatloo@estudiant.upc.edu

Abstract

The outstanding mechanical and tribological properties exhibited by cemented carbides results from the combination of two phases with different local properties. However, direct assessment of the small-scale response of these materials is rather limited in open literature. This is particularly true, regarding experimental analysis on the influence of phase nature, crystal orientation and interfacial adhesion strength on hardness for composites, different from plain WC-Co systems. The present work aims to conduct a systematic micro- and nanomechanical study of the mechanical integrity of two Ti(C,N)-FeNi systems with different ceramic and binder content. It is attempted by combining massive nanoindentation and statistical analysis to extract the intrinsic hardness for each constitutive phase. After that, using the intrinsic hardness for the metallic FeNi binder and the Tabor's equation, the flow stress can be determined. Experimental results are found to validate the evidence of mechanical isotropic for the Ti(C,N) phase. Moreover, they permit to identify and account the strengthening of the plastic-constrained FeNi binder; a critical input parameter for hardness and toughness modeling.

1 Introduction

Cemented carbides contain ceramic and metallic phases, which are absolutely different in terms of chemical nature and mechanical properties. In general, ceramic reinforcements are considered as hardness proof while metallic binder mainly enhances the fracture toughness of these ceramic-metal composites.

Recently there has been growing interest in finding substitute materials for conventional cemented carbides (WC-Co, plain grades usually referred to as hardmetals) because restricted resources of constitutive materials as well as toxicity of Co [1]. Ti(C,N)-FeNi system is proposed as an alternative system for WC-Co, but its potential introduction in industry lies on studies and investigations which can prove that these systems could be a reliable substitution for WC-Co. In this regard, evaluation and analysis of the hardness of Ti(C,N)-FeNi system can lead to microstructural design optimization of new systems.

The present work intends to measure the hardness for each constitutive phases of two different Ti(C,N)-FeNi systems with different ceramic and binder content by means of massive nanoindentation and statistical method [2-6].

2 Materials and experimental procedure

2.1 Sample preparation

Submicron powders used in this study were titanium carbonitride (Ti(C,N), $Ti(C_{0.5},N_{0.5})$ Grade C) and iron (Fe, Fe SM) both provided by H.C. Starck (Germany) and nickel (Ni, Ni 210H) supplied by INCO (Canada).Density of the as-received powders was determined by using a Monosrob Multipycnometer

(Quantachrome Corporation, USA). Laser analyzer (Mastersizer S, Malvern instruments Ltd., UK) and one point N_2 absorption (Monosorb Surface Area, Quantachrome Corporation, USA) were used in order to characterize the particle size and specific surface area respectively.

Table 1. As-received powders characterization.

Characteristics		Powder		
		Ti(C,N)	Fe	Ni
Density ($g \cdot cm^{-3}$)		5.1	7.8	8.9
Size	D_{v50} (μm)	2.1	3.5	1.7
	D_{BET} (μm)	0.4	1.2	0.2
	F_{ag}	5.0	3.0	10
Surface area (m^2/g)		3.0	0.6	4.0

From these powders, high solid content suspensions were formulated using water as dispersion medium [7]. Deionized water with Tetra methyl ammonium hydroxide (TMAH) was used to prepare the suspensions which helps to modify the pH up to 10-11, where surfaces are chemically stable [8, 9]. Then 0.4 wt.% of Polyethylenimine (PEI) was added as dispersant. Ti(C,N) and Fe/Ni (85/15 and 80/20 vol.%) slurries were prepared separately and milled in a ball mill for 1 h, using Si_3N_4 and nylon balls, respectively. When the milling process finished, Ti(C,N) and Fe/Ni suspension was mixed to get the final specimen (Table 2). Once the suspension was prepared, 2 wt.% of Polyvinyl alcohol (PVA) was added as binder [10]. After PVA addition, the suspension remained 20 min under mechanical stirring before it was sprayed.

Table 2. Formulation of the suspensions.

Sample	Vol. %		Composition metal matrix, wt.%	
	Ti(C,N)	Fe/Ni	Fe	Ni
15FeNi	85	15	85	15
20FeNi	80	20	85	15

Stable aqueous suspensions were subjected to spray-dry to obtain agglomerates able to be pressed (spray-dried powder route). To attain this, an atomizer LabPlant SD-05 (North Yorkshire, UK) was used with the main controlled operating parameters being the temperature at inlet and exhaust, which were 190 and 100 ºC, respectively. The slurry pump rate (2 l/h) and the atomizing nozzle design was set to provide spherical agglomerates with high compressibility, able to be shaped by uniaxial pressing [10, 11]. Finally, granules were pressed in a uniaxial die at 600 MPa into cylinders of 16 mm in diameter. All green samples in Table 2 were sintered at 1450ºC for 120 min. in vacuum with a 30 min dwell at 800ºC.

Aiming for microstructural and micromechanical characterization, samples were carefully polished by diamond paste down to 3 μm, followed by a final polishing step with colloidal alumina.

2.2 Microstructural characterization

Figure 1 shows micrographs attained by means of field emission scanning microscopy (FESEM, Jeol 71000F), for Ti(C,N)-FeNi cermets with different binder content. Both microstructures present two distinct phases: a dark grey phase, corresponding to Ti(C,N) particles, and a while light grey one, corresponding to the metallic FeNi matrix.

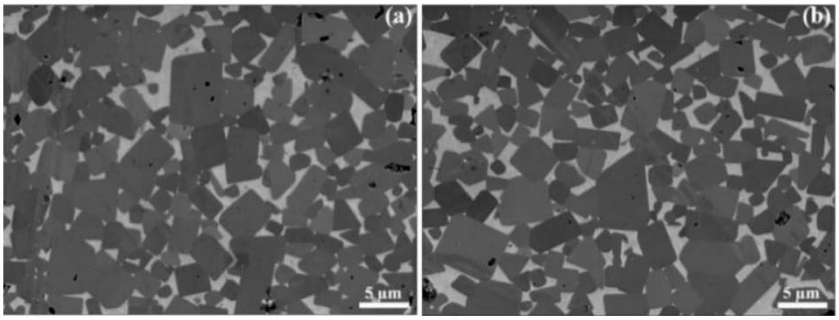

Figure 1. Microstructure of Ti(C,N)-FeNi cermets: (a) 15FeNi and (b) 20FeNi.

Mean grain size of the carbide particles were measured following the linear interception method [12]. Carbide contiguity was estimated by means of best-fit equations, following Roebuck and Almond empirical relations [13-16], but extending them to consider the effect of carbide size [14, 15, 17]. Contiguity values were used to calculate the binder mean free path of the metallic binder for both samples. Table 3 summarizes the microstructural parameters of the composite materials investigated.

Table 3. Microstructural parameters for Ti(C,N)-FeNi cermets.

Sample	Microstructural parameters		
	Mean grain size (µm)	Contiguity	Mean free path (µm)
15FeNi	2.30 ± 0.20	0.47	0.76 ± 0.06
20FeNi	2.23 ± 0.30	0.41	0.95 ± 0.12

2.3 Nanoindentation process

Hardness (*H*) and elastic modulus (*E*) were evaluated for Ti(C,N)-FeNi cermets by means of the instrumented indentation technique. Nanoindentation tests were carried out using a Nanoindenter XP (MTS) unit, which can continuously measure the stiffness modulus. Calibrated diamond Berkovich tip were used to directly extract *H* and *E* by using the Oliver and Pharr method [18, 19]. Two sets of nanoindentation tests were applied on both samples: *i)* one at high penetration depth, to evaluate the *H* and *E* of the composite system at the micrometric length scale; and *ii)* another at small maximum penetration depth to determine the intrinsic *H* of each constitutive phase. In the latter case, small is related to values such to confine the residual imprint and plastic flow inside each constitutive phase. In doing so, an array of 16 imprints (4 by 4) with constant distance of 50 µm between each imprints were applied at 2000 nm penetration depth (or until reaching the maximum applied load, 650 mN) to measure the *H* and *E* of the Ti(C,N)-FeNi composite. On the other hand, to evaluate the intrinsic hardness of each individual phase, 1875 imprints per specimen at 200 nm penetration depth were applied. In this case, imprints were separated by 5 µm distance to avoid any overlapping effect. The *H* directly extracted by using the Oliver and Pharr equations was analyzed by the statistical method proposed by Ulm and co-workers [2-5].

2.4 Statistical method

Statistical method used corresponds to the one proposed by Ulm and co-workers to assess the *H* response of heterogeneous materials. This method considers that investigated material contains various (*i*) constitutive phases, which are absolutely distinct in terms of mechanical properties and chemical nature [2-5]. It also considers that the distribution of mechanical properties, p_i (in the case of *H*) of each constitutive phase follows a Gaussian distribution:

$$p_i = \frac{1}{\sqrt{2 \cdot \pi \cdot \sigma_i^2}} \cdot \exp\left[{(H - H_i)^2} \Big/ {2 \cdot \sigma_i^2} \right] \quad (1)$$

where σ_i is the standard deviation and H_i is the arithmetic mean hardness for number of indentations on different constitutive phases (i). H values were plotted by cumulative distribution function (CDF) while density functions were well fitted by Gaussian distribution. Therefore, corresponding CDF using sigmoid shape error function may be fitted by following equation:

$$CDF = \sum_{i}^{n} \frac{1}{2} \cdot f_i \cdot erf\left[\frac{H - H_i}{\sqrt{2} \cdot \sigma_i}\right] \quad (2)$$

where f_i corresponds to the relative function occupied by each individual phases. Fitting process was set to finish when χ^2 tolerance was less than $1 \cdot 10^{-15}$. Moreover, total volume fraction of constitutive phases was fixed at 1.

3 Results and discussions

3.1 Mechanical properties of the composites

H and E of Ti(C,N)-FeNi composites with different ceramic and binder contents are depicted in Figure 2. As it can be seen, for penetration depths lower than around 500 nm, H and E values are affected by the scale effects (e.g. surface roughness) and tip defect. After that, both curves exhibit a constant value, which yield H and E for each composite system. H for the Ti(C,N)-FeNi samples investigated are found to be 18.0 ± 0.2 GPa and 17.0 ± 0.1 GPa for the 15FeNi and 20FeNi systems, respectively. E ranges between 474 ± 29 GPa and 445 ± 28 GPa for the 15FeNi and 20FeNi. As it is evidenced in Figure 2, H and E decrease when the binder content increases.

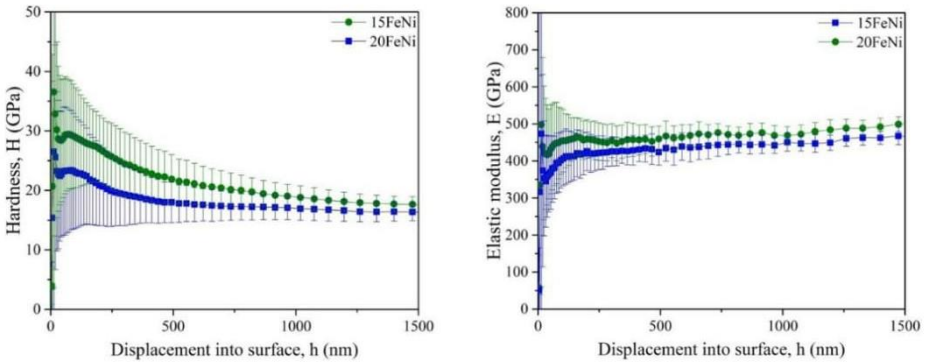

Figure 2. H and E evolution of Ti(C,N)-FeNi cermets as a function of displacement into surface.

3.2 Intrinsic hardness

Experimental results for the constitutive phases are summarized in Table 4. Figure 3a exhibits the experimental hardness data and overlaps the Gaussian simulation for each constitutive phase for the 15FeNi specimen. The same representation has been made for the 20FeNi, but it is not shown here. As it can be seen in this representation, three main peaks are illustrating the intrinsic hardness values for each constitutive phase. Highest value around 33 GPa corresponds to Ti(C,N) particles, while the lowest peak indicates the hardness for metallic binder, ~ 14 GPa. Intermediate peak centered at 24 GPa, may be related to hardness distribution where indentations were implemented on the Ti(C,N) and FeNi interface. Figure 3b exhibits a FESEM image of a small region of indentation array. This micrograph clearly shows that the residual imprints could be completely confined inside the carbide phase when the maximum penetration depth is 200 nm. In this sense, each indentation could be treated as an independent statistical event (see * in Figure 3b).

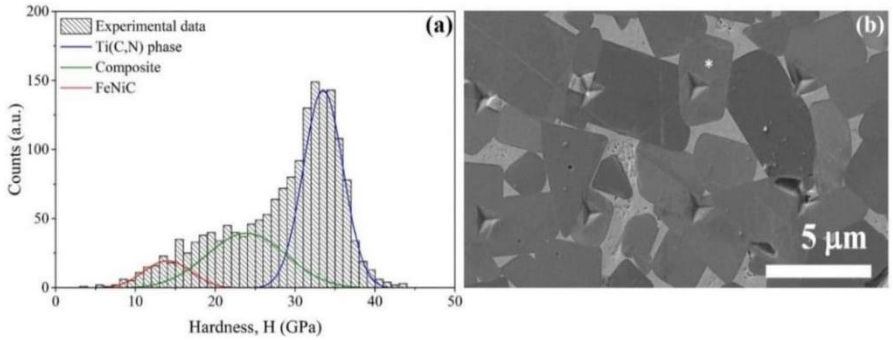

Figure 3. (a) Histogram of hardness with 1GPa of bin size for Ti(C,N)-FeNi cermet. (b) FESEM image of a region of indentation array performed at 200 nm of maximum penetration depth.

Finally, flow stress (σ_{flow}) for the constrained metallic binder was estimated by using Tabor's equation and the intrinsic hardness directly determined from the statistical method. As it is presented in Figure 4; the hardness trend for an individual imprint performed in the FeNi binder presents a hardness plateau and equals to 14.5 GPa, for penetration depths higher than 150 nm. Thus, further analysis was not required. Accordingly, flow stress for the metallic binder is found to range between 3.50 – 4.66 GPa, see table 4.

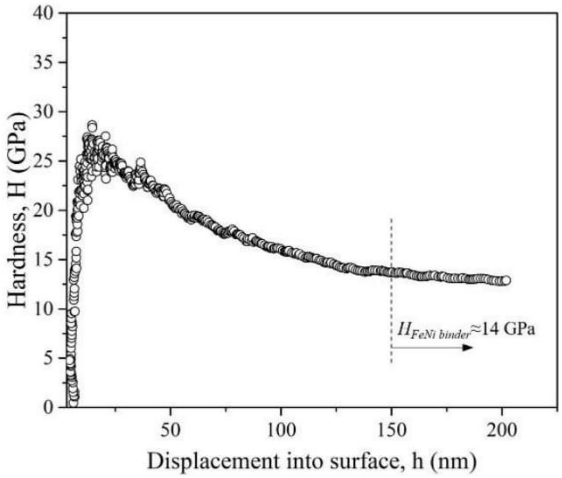

Figure 4. Hardness as a function of displacement into surface for FeNi metallic binder.

Table 4. Summary of the *H* values for each constitutive phase and the σ_{flow} the metallic binder.

Sample	*H* (GPa)			$\sigma_{flow,FeNi}$ (GPa)
	Ti(C,N) particles	Composite	FeNi binder	
15FeNi	33 ± 5	24 ± 8	14 ± 6	3.50 – 4.66
20FeNi	32 ± 2	25 ± 5	14 ± 5	

4 Conclusions

The mechanical behavior of each constitutive phase of Ti(C,N)-FeNi cermet, with different ceramic and binder content, has been evaluated using massive nanoindentation and analyzed following a statistical method. Main conclusions are as follows:

- Hardness and elastic modulus of Ti(C,N)-FeNi composite decrease when the volume fraction of the metallic binder increases.
- Maximum penetration depth of 200 nm could be considered as a suitable nanoindentation testing parameter to attain a successful implementation of the statistical method in Ti(C,N)-FeNi systems.
- Experimental data gathered for Ti(C,N) phase indicates an isotropic behavior regarding hardness.
- The flow stress for the metallic FeNi binder is estimated to range between 3.50-4.66 GPa.

Acknowledgments

The current study was supported by the Spanish Ministerio de Economía y Competitividad (MINECO/FEDER) through Grants MAT2015-70780-C4-3-P, MAT2015-70780-C4-2-P, MAT2015-70780-C4-1-P.

References

[1] B. Gries and L. J. Prakash, "Hard Materials 1: Acute Inhalation Toxicity by Contact Corrosion-The Case of WC-Co," in *European Congress and Exhibition on Powder Metallurgy. European PM Conference Proceedings*, 2007, vol. 1, no. 2, p. 189: The European Powder Metallurgy Association.

[2] G. Constantinides, K. R. Chandran, F.-J. Ulm, and K. Van Vliet, "Grid indentation analysis of composite microstructure and mechanics: Principles and validation," *Materials Science and Engineering: A,* vol. 430, no. 1, pp. 189-202, 2006.

[3] G. Constantinides and F.-J. Ulm, "The nanogranular nature of C–S–H," *Journal of the Mechanics and Physics of Solids,* vol. 55, no. 1, pp. 64-90, 2007.

[4] G. Constantinides, F.-J. Ulm, and K. Van Vliet, "On the use of nanoindentation for cementitious materials," *Materials and structures,* vol. 36, no. 3, pp. 191-196, 2003.

[5] F. J. Ulm, M. Vandamme, C. Bobko, J. Alberto Ortega, K. Tai, and C. Ortiz, "Statistical indentation techniques for hydrated nanocomposites: concrete, bone, and shale," *Journal of the American Ceramic Society,* vol. 90, no. 9, pp. 2677-2692, 2007.

[6] J. Roa *et al.*, "Intrinsic hardness of constitutive phases in WC–Co composites: Nanoindentation testing, statistical analysis, WC crystal orientation effects and flow stress for the constrained metallic binder," *Journal of the european ceramic society,* vol. 35, no. 13, pp. 3419-3425, 2015.

[7] J. Escribano, B. Ferrari, P. Alvaredo Olmos, E. Gordo Odériz, and A. Sánchez-Herencia, "Colloidal processing of Fe-based metalceramic composites with high content of ceramic reinforcement," *Boletín Sociedad Española De Cerámica y Vidrio 52,* 2013.

[8] J. Escribano, J. García, P. Alvaredo, B. Ferrari, E. Gordo, and A. J. Sanchez-Herencia, "FGM stainless steel-Ti (C, N) cermets through colloidal processing," *International Journal of Refractory Metals and Hard Materials,* vol. 49, pp. 143-152, 2015.

[9] P. Parente, A. Sanchez-Herencia, M. Mesa-Galan, and B. Ferrari, "Functionalizing Ti-surfaces through the EPD of hydroxyapatite/nanoY2O3," *The Journal of Physical Chemistry B,* vol. 117, no. 6, pp. 1600-1607, 2012.

[10] R. Neves, B. Ferrari, A. Sanchez-Herencia, and E. Gordo, "Colloidal approach for the design of Ti powders sinterable at low temperature," *Materials Letters,* vol. 107, pp. 75-78, 2013.

[11] M. Dios, Z. Gonzalez, P. Alvaredo, R. Bermejo, E. Gordo, and B. Ferrari, "Colloidal processing of Ti(C,N)-based cermets from commercial powders."

[12] "Metallographic Determination of Microstructure. Part 2: Measurement of WC Grain Size,," in *ISO 4499-2: 2008 Hardmetals*: Geneva, 2008.

[13] B. Roebuck and E. Almond, "Deformation and fracture processes and the physical metallurgy of WC–Co hardmetals," *International Materials Reviews,* vol. 33, no. 1, pp. 90-112, 1988.

[14] Y.Torres, "Comportamiento a fractura y fatiga de carburos cementados WC– Co, ," PhD thesis, Universitat Politècnica de Catalunya, Barcelona, 2002.

[15] D. Coureaux, "Comportamiento mecánico de carburos cementados WC– Co: influencia de la microestructura en la resistencia a la fractura, la sensibilidad a la fatiga y la tolerancia al da ño

inducido bajo solicitaciones de contacto," PhD thesis, Universitat Politècnica de Catalunya, Barcelona, 2012.

[16] H. Exner, "Physical and chemical nature of cemented carbides," *International metals reviews,* vol. 24, no. 1, pp. 149-173, 1979.

[17] J. Tarragó, J. Roa, V. Valle, J. Marshall, and L. Llanes, "Fracture and fatigue behavior of WC–Co and WC–CoNi cemented carbides," *International Journal of Refractory Metals and Hard Materials,* vol. 49, pp. 184-191, 2015.

[18] W. C. Oliver and G. M. Pharr, "An improved technique for determining hardness and elastic modulus using load and displacement sensing indentation experiments," *Journal of materials research,* vol. 7, no. 06, pp. 1564-1583, 1992.

[19] W. C. Oliver and G. M. Pharr, "Measurement of hardness and elastic modulus by instrumented indentation: Advances in understanding and refinements to methodology," *Journal of materials research,* vol. 19, no. 01, pp. 3-20, 2004.